

# G protein $\beta\gamma$ subunit interaction with the dynein light-chain component Tctex-1 regulates neurite outgrowth

Pallavi Sachdev<sup>1</sup>, Santosh Menon<sup>1</sup>,  
David B Kastner<sup>1,5</sup>, Jen-Zen Chuang<sup>2</sup>,  
Ting-Yu Yeh<sup>2,6</sup>, Cecilia Conde<sup>3</sup>,  
Alfredo Caceres<sup>3</sup>, Ching-Hwa Sung<sup>2,4</sup>  
and Thomas P Sakmar<sup>1,\*</sup>

<sup>1</sup>Laboratory of Molecular Biology and Biochemistry, The Rockefeller University, New York, NY, USA, <sup>2</sup>Department of Ophthalmology, Weill Medical College of Cornell University, New York, NY, USA, <sup>3</sup>INIMEC-CONICET, Cordoba, Argentina and <sup>4</sup>Department of Cell and Developmental Biology, Weill Medical College of Cornell University, New York, NY, USA

**Tctex-1, a light-chain component of the cytoplasmic dynein motor complex, can function independently of dynein to regulate multiple steps in neuronal development. However, how dynein-associated and dynein-free pools of Tctex-1 are maintained in the cell is not known. Tctex-1 was recently identified as a G $\beta\gamma$ -binding protein and shown to be identical to the receptor-independent activator of G protein signaling AGS2. We propose a novel role for the interaction of G $\beta\gamma$  with Tctex-1 in neurite outgrowth. Ectopic expression of either Tctex-1 or G $\beta\gamma$  promotes neurite outgrowth whereas interfering with their function inhibits neurite outgrowth. Using embryonic mouse brain extracts, we demonstrate an endogenous G $\beta\gamma$ -Tctex-1 complex and show that G $\beta\gamma$  co-segregates with dynein-free fractions of Tctex-1. Furthermore, G $\beta$  competes with the dynein intermediate chain for binding to Tctex-1, regulating assembly of Tctex-1 into the dynein motor complex. We propose that Tctex-1 is a novel effector of G $\beta\gamma$ , and that G $\beta\gamma$ -Tctex-1 complex plays a key role in the dynein-independent function of Tctex-1 in regulating neurite outgrowth in primary hippocampal neurons, most likely by modulating actin and microtubule dynamics.**

*The EMBO Journal* (2007) **26**, 2621–2632. doi:10.1038/sj.emboj.7601716; Published online 10 May 2007

**Subject Categories:** signal transduction

**Keywords:** AGS; dynein; heterotrimeric G protein; neurite outgrowth

## Introduction

Signaling pathways that lead to neurite outgrowth and the establishment of neuronal polarity remain poorly understood. However, dynamic rearrangements of microtubules and actin filaments at the tips of growing axons are observed during neurite sprouting and elongation, suggesting that molecules that coordinate microtubule and actin microfilament dynamics play key roles in neurite extension and neuronal polarity determination (Fukata *et al*, 2002; Baas and Buster, 2004). Cytoplasmic dynein light-chain component, Tctex-1, was demonstrated recently to play key roles in initial neurite sprouting, axonal specification and elongation of hippocampal neurons in culture (Chuang *et al*, 2001, 2005). Cytoplasmic dynein is a microtubule-based, minus-end-directed motor complex involved in various cellular activities, including retrograde trafficking in neurons, Golgi maintenance, breakdown of the nuclear envelope and mitosis (Hirokawa, 1998; Sakato and King, 2004). Dynein comprises two ~530 kDa heavy chains (DHCs) with ATPase and motor activities, two or three 74-kDa intermediate chains (DICs), and a group of accessory polypeptides including light intermediate chains and light chains (DLCs) (Vallee *et al*, 2004). DICs link accessory proteins, including the DLCs and the dynactin complex, to the DHC (Waterman-Storer *et al*, 1995; King, 2000). Three distinct DLC families have been identified: Tctex-1 (DYNTL1; Pfister *et al*, 2005), LC8 and LC7/Roadblock (Vallee *et al*, 2004).

Several lines of evidence suggest that Tctex-1 might function independently from dynein. First, there is strong biochemical evidence that a dynein-free pool of Tctex-1 exists independently of the dynein complex-associated Tctex-1 (Tai *et al*, 1998). Secondly, Tctex-1 is abundantly expressed in postmitotic, young neurons and was demonstrated recently to play a key role in neurite outgrowth in hippocampal neurons in culture (Chuang *et al*, 2001, 2005). Cultured hippocampal neurons develop multiple abnormally long neurites when Tctex-1 is overexpressed and fail to develop neurites when Tctex-1 is suppressed (Chuang *et al*, 2005). The function of Tctex-1 in neurite outgrowth was demonstrated to be dynein independent, since a mutant of Tctex-1 (Tctex-1 T94E), which failed to bind to DIC and therefore could not get incorporated into the dynein complex, induced a similar phenotype as the wild-type Tctex-1 protein (Chuang *et al*, 2005). Finally, Tctex-1 interacts with proteins besides DIC, including rhodopsin (Tai *et al*, 1999), parathyroid hormone receptor (PTHr) (Sugai *et al*, 2003), poliovirus receptor CD155 (Ohka *et al*, 2004), Herpes virus capsid protein VP26 (Douglas *et al*, 2004), bone morphogenetic receptor type II (BMPRII) (Machado *et al*, 2003), the voltage-dependent anion channel (VDAC) (Schwarzer *et al*, 2002), Fyn kinase (Kai *et al*, 1997; Mou *et al*, 1998) and Trk neurotrophin receptor (Yano *et al*, 2001; Yano and Chao, 2004). How dynein-associated and dynein-free pools of Tctex-1 are main-

\*Corresponding author. Laboratory of Molecular Biology and Biochemistry, The Rockefeller University, 1230 York Avenue, Box 187, New York City, NY 10021, USA. Tel.: +1 212 327 8288; Fax: +1 212 327 7904; E-mail: sakmar@rockefeller.edu

<sup>5</sup>Present address: Stanford University Medical School, Palo Alto, CA 94305, USA

<sup>6</sup>Present address: Johns Hopkins University, Baltimore, MD 21218, USA

Received: 16 August 2006; accepted: 12 April 2007; published online: 10 May 2007

tained in the cell and how the assembly of Tctex-1 into the dynein complex is regulated is not known.

Tctex-1 was independently identified as an activator of G protein signaling 2 (AGS2), a receptor-independent activator of heterotrimeric guanine-nucleotide-binding regulatory proteins (G proteins), in a functional yeast screen in yeast (Takesono *et al*, 1999). AGS molecules can generally be divided into three subgroups: those that directly activate Gα, those that modulate Gα-Gβγ interaction by binding to Gα, and those that modulate Gα-Gβγ interaction by binding to Gβγ (Lanier, 2004). These AGS molecules have since demonstrated novel, non-canonical roles for G protein subunits in cell development and differentiation. For example, silencing of AGS3, a receptor-independent activator of Gβγ signaling, resulted in defects in mitotic spindle orientation and cleavage plane determination of neural progenitors in the developing neocortex demonstrating a novel role for G proteins in regulating neuronal cell fate (Sanada and Tsai, 2005).

AGS2/Tctex-1 was reported to bind Gβγ, but the molecular mechanism and functional consequences of the putative Tctex-1-Gβγ interaction have remained unknown (Takesono *et al*, 1999). Here, we studied the role of Gβγ in regulating the dynein-independent function of Tctex-1 in neurogenesis. An endogenous Gβγ-Tctex-1 complex can be isolated from embryonic brain lysates and Gβ overlaps with the 'dynein-free' Tctex-1 in cell fractionation experiments. Subcellular distribution of Gβγ and Tctex-1 overlap in the cell bodies as well as the growth cones of nascent axons in stage 3 primary cultured hippocampal neurons. Both Tctex-1 and Gβγ overexpression elicit similar phenotypes in primary hippocampal neurons. Interfering with Gβγ function inhibits neurogenesis and diminishes the ability of Tctex-1 to induce neurite outgrowth. All known Gβ isoforms contain an identical

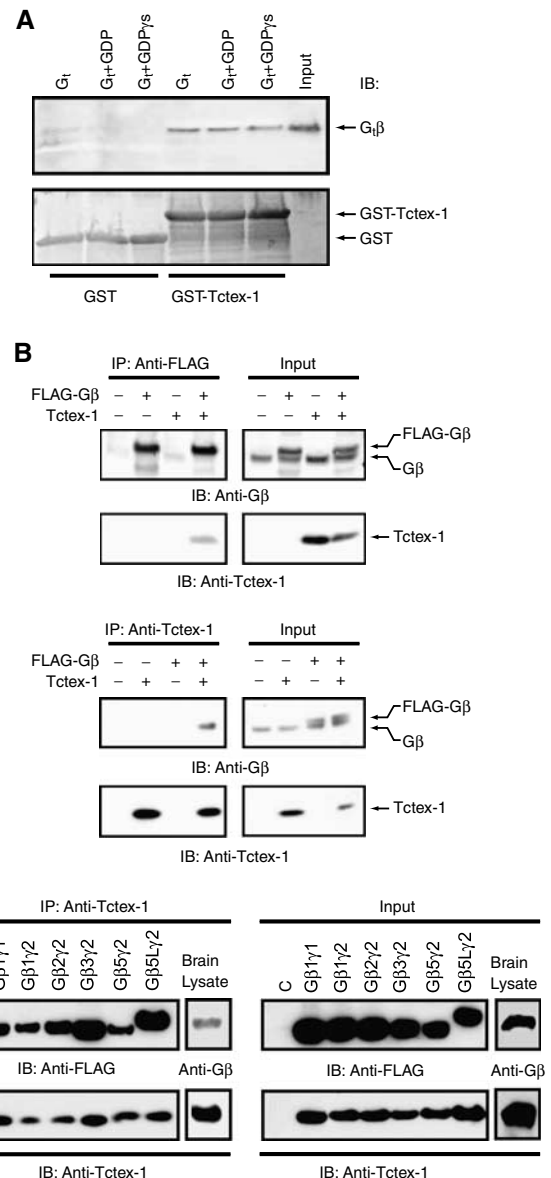
consensus Tctex-1-binding motif first described in DIC (Mok *et al*, 2001). We show that full-length Gβ1, as well as a Gβ-peptide corresponding to the Tctex-1-binding region of Gβ1, compete with DIC for Tctex-1 binding. We propose that Gβγ binds to Tctex-1 to regulate the dynein-independent pool of Tctex-1 and its incorporation into the dynein motor complex. Finally, we demonstrate that Gβγ-Tctex-1 complex plays a key role in neurogenesis in an established model of hippocampal neuron differentiation.

## Results

### Characterization of Gβγ-Tctex-1 interaction

Tctex-1 was shown to interact specifically with Gβγ and not with the Gα subunit of heterotrimeric G proteins (Takesono *et al*, 1999). We confirmed the interaction of Gβγ with Tctex-1 using purified components. We generated GST-tagged Tctex-1 and purified visual G protein transducin, G<sub>t</sub>αβγ. GST-Tctex-1 was incubated with G<sub>t</sub>αβγ and the bound G<sub>t</sub>βγ subunit was detected using an anti-Gβ antibody. As shown in Figure 1A, GST-Tctex-1 but not GST alone, specifically bound

**Figure 1** Gβγ interacts with Tctex-1. **(A)** Transducin G<sub>t</sub>αβ1γ1 (G<sub>t</sub>) interacts with GST-fused Tctex-1. GST alone (lanes 1–3) or GST-fused Tctex-1 (lanes 4–6) (300 nM) were incubated with G<sub>t</sub> (40 nM) (lanes 1 and 4), plus 10 μM GDP (lanes 2 and 5) or plus 10 μM GTPγS and 5 mM MgCl<sub>2</sub> (lanes 3 and 6). Purified G<sub>t</sub> was loaded as a control in lane 7. The bound samples were analyzed by SDS-PAGE followed by immunoblotting (IB) for Gβ using anti-Gβ antibody (top panel). A Coomassie blue-stained gel in the bottom panel shows that equal amounts of the GST and GST-Tctex-1 were used. **(B)** Gβγ and Tctex-1 co-IP in HEK cells. HEK cells were transfected with FLAG-tagged Gβ1 and Tctex-1 cDNAs as indicated and cell lysates were immunoprecipitated (IP) with anti-Tctex-1 antibody (top panel) or with anti-FLAG antibody (bottom panel) and subjected to SDS-PAGE, followed by Western blot analysis (IB) using anti-Gβ and anti-Tctex-1 antibodies. A 20 μg weight of total cell lysate was analyzed as input (right half of each panel) to show expression levels of Gβ and Tctex-1. The doublet seen in the anti-Gβ blots correspond to the endogenous Gβ and the FLAG-tagged Gβ proteins. **(C)** Tctex-1 interacts with several overexpressed Gβ isoforms, and with endogenous Gβ in brain lysates. HEK293 cells were cotransfected with FLAG-tagged Gβ1, β2, β3, β5 or β5L, along with Gγ1 or Gγ2 and Tctex-1 expression vectors. Tctex-1 was IP with anti-Tctex-1 antibody and the immunocomplexes were analyzed by Western blotting using anti-Tctex-1 antibody to detect Tctex-1 and anti-FLAG antibody to detect the FLAG-tagged Gβ subunits that co-IP with Tctex-1. Endogenous Tctex-1 was immunoprecipitated from E15 embryonic mouse brain lysate using anti-Tctex-1 antibody and analyzed by Western blotting for Tctex-1 and the associated brain Gβ subunit using anti-Tctex-1 and anti-pan Gβ antibody, respectively. A 20 μg weight of total cell lysate was analyzed by as input to show protein expression levels of Tctex-1, FLAG-tagged Gβ and endogenous Gβ using anti-Tctex-1, anti-FLAG and anti-pan Gβ antibodies, respectively. All images are representative of three independent experiments.



G $\beta$ . We also studied the G $\beta$ -Tctex-1 interaction in a mammalian cell expression system. We cotransfected human embryonic kidney (HEK) cells with Tctex-1 and G $\beta$ 1 expression plasmids. Confirming the *in vitro* data, we showed that Tctex-1 could robustly co-immunoprecipitate (co-IP) with G $\beta$  (Figure 1B). Tctex-1 did not co-IP with overexpressed G $\alpha$  in HEK cells (data not shown). The G $\beta$  subunit consists of six different isoforms, including G $\beta$ 1 through 5 and a splice variant of G $\beta$ 5 called G $\beta$ 5L (long form). G $\beta$ 1-4 are about 80% identical to each other, whereas G $\beta$ 5 is only about 50% identical to the others. As shown in Figure 1C, all FLAG-tagged G $\beta$  subunits (G $\beta$ 1, 2, 3, 5 and 5L) co-immunoprecipitated with Tctex-1 using an anti-Tctex-1 antibody. The expression of G $\gamma$ 1 or G $\gamma$ 2 together with G $\beta$ 1 did not affect the ability of Tctex-1 to associate with G $\beta$ 1. G $\gamma$ 1 and G $\gamma$ 2 expression was confirmed by stripping and reprobing the membranes with anti-G $\gamma$ 1 and anti-G $\gamma$ 2 antibodies, respectively (data not shown). Even though both G $\beta$  and Tctex-1 are expressed in HEK 293 cells, we failed to co-IP a native endogenous G $\beta$ -Tctex-1 complex from these cells. Since Tctex-1 is abundantly expressed in postmitotic young neurons and several G $\beta$  combinations are found in brain, we employed embryonic mouse brain lysates in pull-down assays (Chuang *et al*, 2001). As shown in Figure 1C, we were able to pull down G $\beta$  along with Tctex-1, demonstrating a native endogenous G $\beta$ -Tctex-1 complex in mouse embryonic brain lysate.

To map the G $\beta$ -binding site on Tctex-1, we constructed N- and C-terminal truncation mutants of Tctex-1. FLAG-tagged full-length Tctex-1 and various truncation mutants of Tctex-1 were cotransfected with G $\beta$ 1 in HEK cells (Figure 2A). As shown in Figure 2B, full-length and the N-terminal truncated mutants of Tctex-1 were able to co-IP G $\beta$ , whereas the C-terminal truncation mutant of Tctex-1, 1-92, which is missing the last 21 amino acids of Tctex-1, failed to co-IP G $\beta$  (Figure 2B). Taken together, these results suggest that the C-terminal tail of Tctex-1 is required for the G $\beta$ -Tctex-1 interaction.

### Consensus binding motif on G $\beta$ is required for Tctex-1 binding

An 11-amino-acid peptide derived from DIC was used to identify residues on Tctex-1 that are involved in the DIC-Tctex-1 interaction (Mok *et al*, 2001). Comparison of this peptide sequence of DIC with sequences of other Tctex-1 target proteins helped to identify a motif of basic residues, R/K-R/K-X-X-R/K, as a consensus Tctex-1-binding motif (Mok *et al*, 2001). Additionally, a second Tctex-1-binding motif, V-S-K/H-T/S-X-V/T-T/S-N/Q-V, has also been identified in a subset of Tctex-1-interacting proteins (Sugai *et al*, 2003). We found a potential Tctex-1-binding motif in all six G $\beta$  subunits, which maps to the outermost  $\beta$ -strand of the seventh blade of the G $\beta$  propeller (Figure 3A and B). We generated a G $\beta$ -peptide corresponding to amino acids 40-57 of G $\beta$ 1, which includes the basic Tctex-1-binding motif and surrounding residues either with no tag or with a thiol-specific, environmentally-sensitive, fluorescent compound, MIANS. We performed fluorescence anisotropy measurements to determine the binding affinity of the G $\beta$ -peptide to Tctex-1. Keeping the MIANS-labeled G $\beta$ -peptide constant and adding increasing concentrations of purified Tctex-1, we observed enhanced binding, which leveled off at high concentrations of G $\beta$ -peptide (Figure 3C). The experimentally determined  $K_d$  for the G $\beta$ -peptide-Tctex-1 interaction was 1.35  $\mu$ M.

We further dissected the binding motif to identify which particular residues within the binding motif are critical for the G $\beta$ -Tctex-1 interaction. The cluster of basic residues within the Tctex-1-binding motif (R/K-R/K-X-X-R/K) prompted us to evaluate the role of charge-based regulation of the interaction. We generated site-directed mutants of the Tctex-1-binding motif in G $\beta$ , where the Arg residues were replaced either individually or in combination, and tested their ability to interact with Tctex-1 in co-IP experiments. In accordance with our hypothesis, we found that mutation of all three basic residues (R48, R49 and R52) to alanines within the full-length

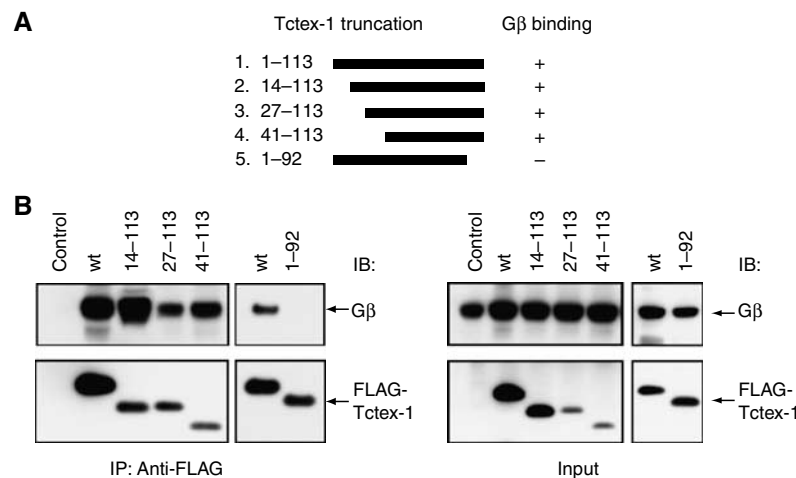


**Figure 2** Mapping of the G $\beta$ -binding domain of Tctex-1. (A) Schematic representation of the N- and C-terminal truncation mutants of Tctex-1 used in the mapping of the G $\beta$ -binding domain of Tctex-1. (B) C-terminal region of Tctex-1 is required for G $\beta$  binding. HEK cells were cotransfected with the indicated truncation mutants of FLAG-tagged Tctex-1, along with G $\beta$  cDNAs. Tctex-1 and its mutants were immunoprecipitated with anti-FLAG antibody and the immunocomplexes were analyzed by Western blotting with anti-G $\beta$  antibody (top panels) and anti-FLAG antibody to detect FLAG-tagged Tctex-1 (bottom panels). The expression level of each protein was analyzed by direct Western using 20  $\mu$ g of total cell lysate as input. This is a representative image of at least three independent experiments.

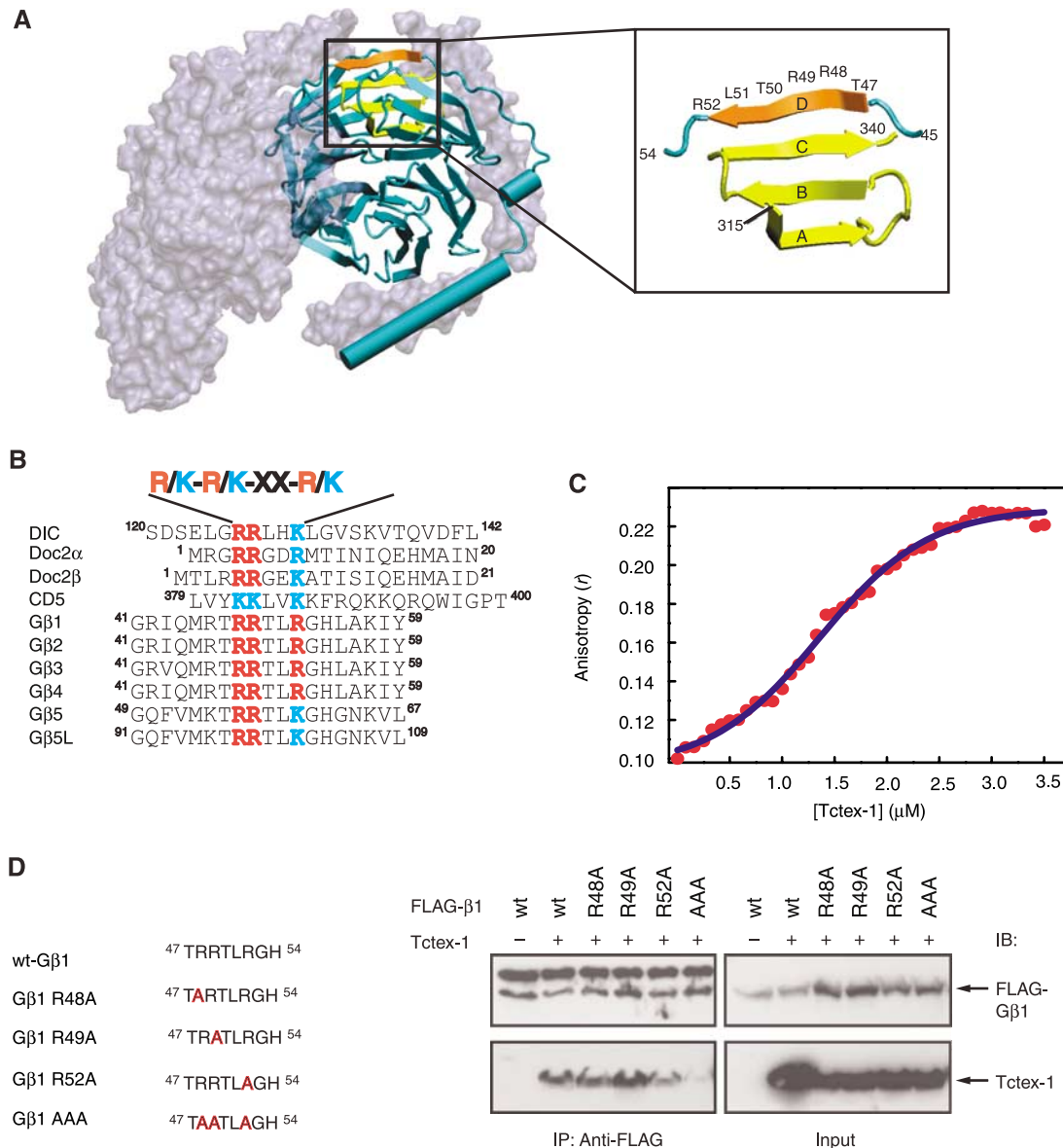


**Figure 3** Analysis of the Tctex-1-interacting motif on Gβ. (A) Structure of heterotrimer Gαβγ highlighting the Tctex-1-binding motif in Gβ. Gα and Gγ (gray) are shown as molecular surface representation, whereas Gβ (cyan) is shown as a secondary structure cartoon. Four β-strands that make up blade 7 of the Gβ propeller are highlighted (β-strands A–C in yellow and β-strand D in orange, left panel). Expanded region (right panel) shows the region of Gβ involved in the formation of blade 7. C-terminal residues 315–340 (yellow) form the A, B and C β-strands, whereas N-terminal residues 47–52 (orange) form the outermost D β-strand of this blade. Residues 47–52 comprise the consensus R/K-R/K-X-X-R/K Tctex-1-binding motif. Image created using VMD software (Humphrey *et al*, 1996). Crystal coordinates obtained from PDB file 1GOT (Lambright *et al*, 1996). (B) Consensus sequence R/K-R/K-X-X-R/K found in various Tctex-1-interacting proteins. (C) Fluorescence anisotropy of MANS-labeled Gβ-peptide in the presence of Tctex-1. Tctex-1 was titrated to the MANS Gβ-peptide, whose concentration was maintained at 0.7 μM. With increasing concentration of Tctex-1, there was an enhancement in the anisotropy value, indicative of specific binding of the peptide to the protein. In addition, the plot showed a sigmoidal curve, indicative of cooperative binding. Each data point is an average of five readings with standard error less than 5%. The  $K_d$  value for the Tctex-1-Gβ-peptide interaction from nonlinear regression analysis was calculated to be 1.35 μM. (D) Reduced interaction of Gβ AAA mutant with Tctex-1. HEK cells were cotransfected with Tctex-1 and the indicated FLAG-tagged Gβ mutants. The AAA Gβ1 mutant, wherein all three Arg residues (R48, R49 and R52) within the consensus Tctex-1-binding motif are mutated to alanine, showed significantly reduced ability to co-IP Tctex-1. The upper band observed in the top left panel of the anti-FLAG IP corresponds to the IgG heavy chain. This image is representative of three independent experiments.

Gβ protein (Gβ1 AAA) significantly decreased the ability of Gβγ to interact with Tctex-1 (Figure 3D).

### Gβγ and Tctex-1 distribution overlaps in cultured hippocampal neurons

Tctex-1 was recently shown to regulate neurite outgrowth in primary hippocampal neurons (Chuang *et al*, 2005). We decided to investigate whether the endogenous Gβγ-Tctex-1

complex, isolated from mouse brain lysates, could play a role in Tctex-1-induced neurogenesis. To this end, we first examined the expression pattern of Gβ in cultured primary hippocampal neurons. Primary hippocampal neurons adopt the characteristic polarized morphology in a well-defined sequence of developmental stages (Dotti *et al*, 1988; Fukata *et al*, 2002). Within 24 h of plating, hippocampal neurons send out several processes of relatively equal length (stage 2).

Even though phenotypically the neurons still appear non-polarized, proteins known to be involved in cell polarization already start to display a polarized distribution pattern (Bradke and Dotti, 2000; Fukata *et al*, 2002; Banker, 2003; Schwamborn and Puschel, 2004). At this stage, Gβ displays diffuse labeling throughout the cell body and the minor processes (Figure 4A–C). As the neurons develop through stages 2–3 and reach stage 3, they adopt the final differentiated polarized neuronal phenotype with one long neurite (the nascent axon) and several minor processes. Approximately 40% of stage 3 neurons examined ( $n > 50$ ) displayed Gβ immunoreactivity in the central region of the axonal growth cones (Figure 4D–K), whereas the remaining neurons failed to show an enhanced labeling intensity of Gβ in the growth cones (Figure 4L–N).

We then examined the expression patterns of Gβ and Tctex-1 in hippocampal neurons of various stages. Tctex-1 and Gβ are expressed essentially homogeneously throughout the cell body and processes of stage 2 neurons (Figure 5Aa–c). As the neurons develop through stages 2–3, Gβ and Tctex-1 continue to overlap in the perinuclear Golgi region within the cell body. We also observed a strong colocalization of Tctex-1 and Gβ within the axonal growth cones of majority of stage 3 neurons (70%,  $n = 100$ ) (Figure 5Ad–i and 5B).

#### Role of Gβγ and Tctex-1 in neuronal differentiation

To study the role of Gβγ in hippocampal neuronal differentiation, we used a Gβγ-specific antagonist, βARKct, to perform loss-of-function experiments. βARKct contains the Gβγ-binding domain of β-adrenergic receptor kinase 1 and when

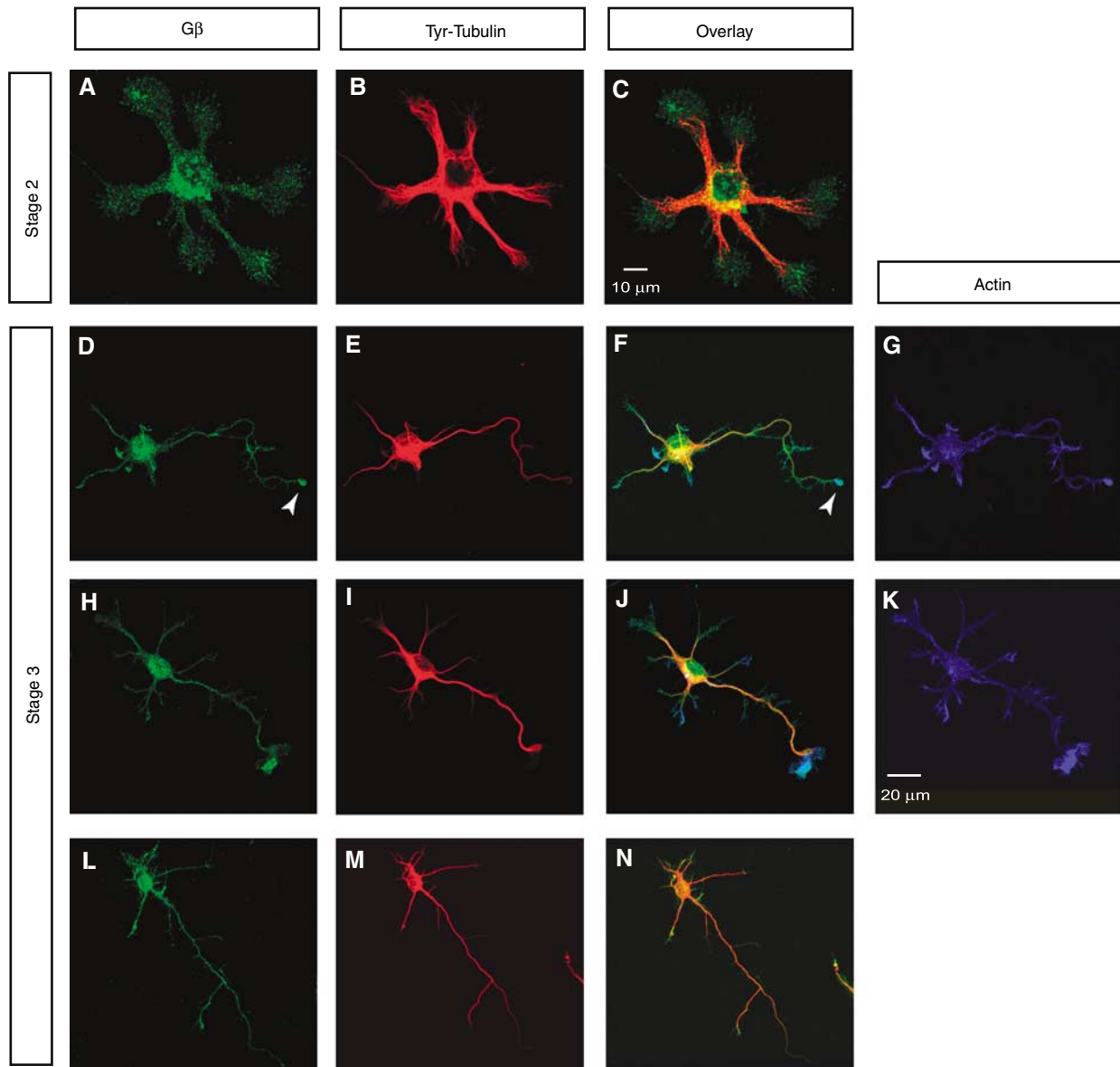


**Figure 4** Expression pattern of Gβ in various stages of cultured primary hippocampal neuron differentiation. Gβ distributes diffusely throughout the cell body and the minor processes in stage 2 neurons (A–C). As the neurons develop through stages 2–3 and reach stage 3 and adopt the well-differentiated neuronal phenotype, Gβ shows two distinct labeling patterns. Approximately 40% of stage 3 neurons ( $n > 50$ ) showed Gβ labeling in the central region of the axonal growth cone (D–K). An example of a stage 3 neuron that failed to show any detectable enhancement of Gβ in the growth cones is represented (L–N). Neurons were colabeled for Gβ (green in A, D, H and L), Tyr-Tubulin (red in B, E, I and M) and actin (blue in G and K). Overlaid images are shown in C, F, J and N. Scale bars equal 10 μm in panels (A–C) and 20 μm in panels (D–N).

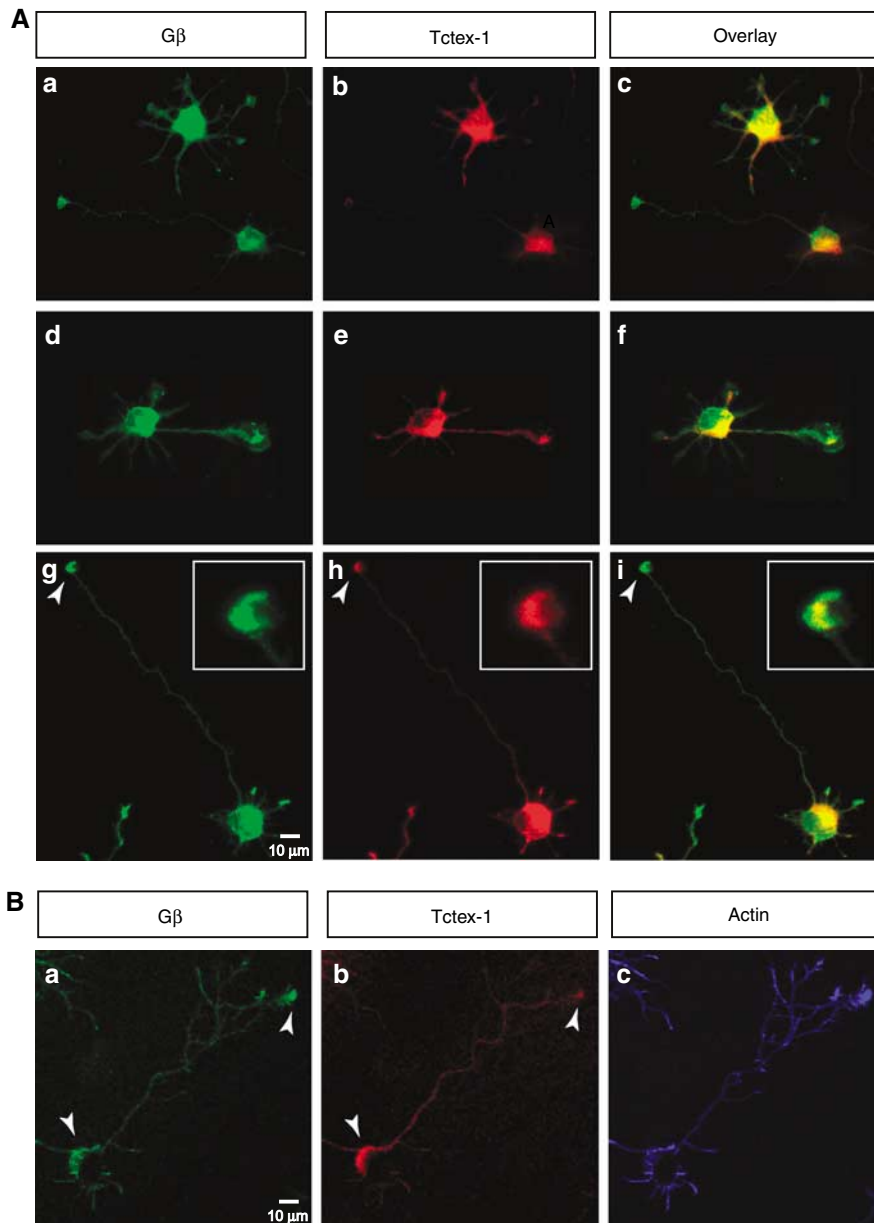


**Figure 5** Overlapping distribution of Tctex-1 and Gβ in hippocampal neurons. **(A)** Cultured hippocampal neurons in various stages of differentiation were colabeled for Gβ (green in a, d and g) and Tctex-1 (red in b, e and h). The overlaid images are shown in c, f and i. Gβ and Tctex-1 show homogenous expression within the cell body and all the neurites in typical stage 2 cells (a–c). As the neurons progress through stage 3, Gβ and Tctex-1 continue to overlap within the cell body, but in addition, show strong co-distribution at the growth cones of the future axon (a–i). Majority of the stage 3 neurons examined (70%,  $n = 100$ ) (a–f) show enhanced colabeling of Gβ and Tctex-1 in axonal growth cones as compared with the minor neurites that do not show an enrichment of Gβ or Tctex-1 at the tips. A small subset of the stage 3 neurons examined (30%,  $n = 100$ ) continued to show colabeling of Gβ and Tctex-1 in the cell body and at the axonal growth cones, and also showed some colabeling at the tips of the minor neurites (g–i). A magnified view of the growth cone of a stage 3 neuron is shown in the inset (g–i). Greater than 100 individual neurons were examined. Scale bar equals 10 μm (a–i) and 3 μm in the magnified insets (g–i). **(B)** Confocal image of a representative stage 3 neuron shows perinuclear, cytoplasmic staining for Gβ and Tctex-1 within the cell body and an enrichment at the tips of some of the axonal growth cones (panels A–C). Scale bar equals 10 μm.

expressed in intact cells, it inhibits Gβγ-dependent signaling by binding to and sequestering Gβγ (Koch *et al*, 1994). Hippocampal neurons transfected with EGFP expression vector alone were indistinguishable from non-transfected cells and developed normally through stage 2 and stage 3 (Figure 6A). Quantification of the different stages showed that a significant fraction of neurons transfected with EGFP alone were found in stage 2 (52%) and stage 3 (40%) (Table I). To study the effect of βARKct on neurite outgrowth,

hippocampal neurons were transfected either 2 h after plating or 12 h after plating with expression vectors for βARKct together with EGFP (Figure 6B and Supplementary Figure 1). As seen in Figure 6B, neurons that were transfected with the EGFP plus βARKct 2 h after plating failed to develop neurites and seemed to be arrested in stage 1 (78%) (Figure 6B and Supplementary Figure 1). The neighboring, untransfected cells (observed within the same field) appear healthy and proceed normally through development

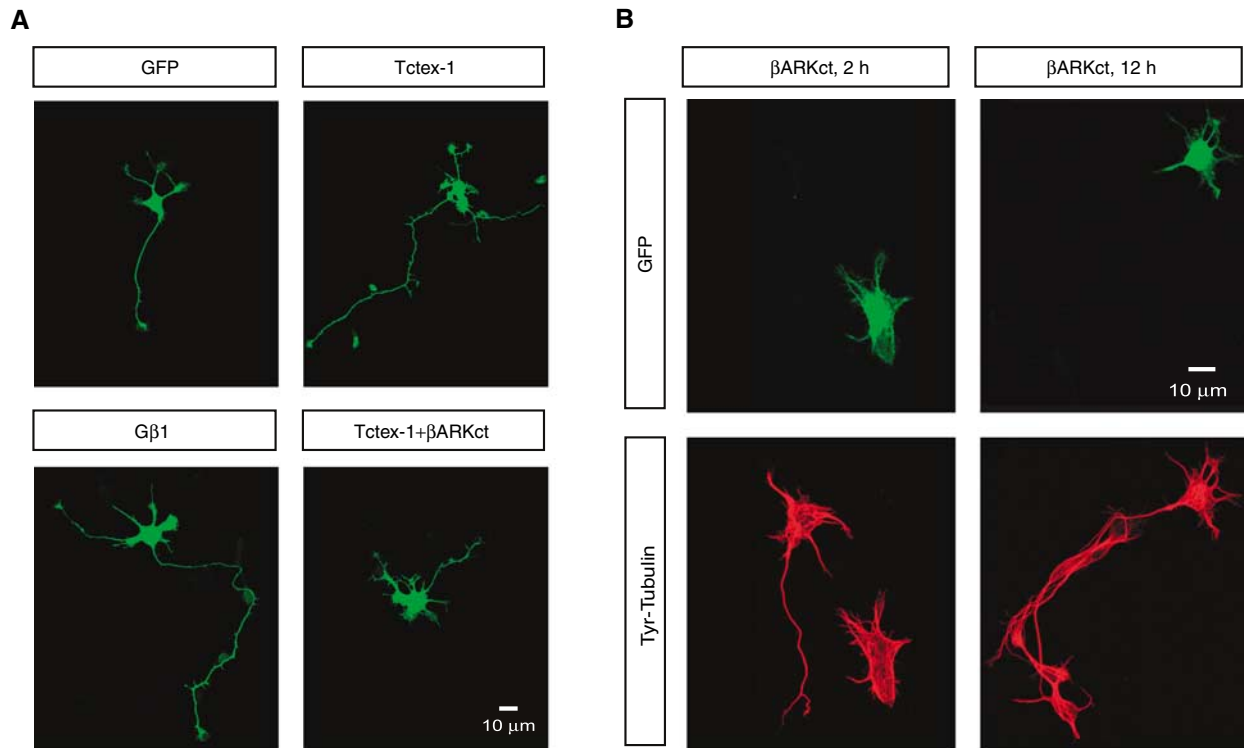


**Figure 6** Role of Gβγ and Tctex-1 in neuronal differentiation. (A) Ectopic expression of Gβ1 and Tctex-1 induces multiple, long neurites in hippocampal neurons. Hippocampal neurons were transfected as indicated, with expression vectors for GFP, GFP + FLAG-Gβ1, GFP + FLAG-Tctex-1 and GFP + Tctex-1 + βARKct 2 h after plating. The transfected neurons were fixed and processed for GFP fluorescence 24 h after transfection. (B) Expression of Gβγ-sequestering reagent, βARKct inhibits neurite outgrowth. Hippocampal neurons were transfected either 2 h or 12 h after plating, with expression vectors for GFP and βARKct and analyzed 24 h after transfection for GFP expression (green) and Tyr-Tubulin labeling (red). βARKct expression results in arresting the cells in stage 1 when transfected 2 h after plating and in stage 2 when transfected 12 h after plating. Note that, under both conditions, the untransfected cells within the same field appear healthy and have reached stage 3. The images shown here are representative of three independent transfections. Quantification of the images from these transfections is shown in Table I.

**Table I** Quantitative analyses of morphological changes of transfected neurons

Overexpressed protein	% cells (stage 1)	% cells (stage 2)	% cells with a single neurite (stage 3)	% cells with multiple neurites >70–80 μm
GFP alone	8 ± 4	52 ± 8	40 ± 6	0.6 ± 01
βARKct	78 ± 6*	17 ± 3*	4 ± 2*	ND
FLAG-Gβ1	2 ± 1	36 ± 9*	42 ± 14	22 ± 6*
FLAG-Tctex1	2 ± 1	24 ± 8*	28 ± 6	38 ± 8*
FLAG-Tctex1 + βARKct	10 ± 4	38 ± 4*	40 ± 12	12 ± 6*

Cells were transfected at 2 h after plating and fixed 24 h later. Each transfection received 1 μg of GFP expressing vector for visualizing the transfected cells. For all other constructs, 2 μg of plasmid were typically used. The total amount of DNA added was kept constant by adding appropriate amount of control vector. A neurite longer than 70–80 μm was considered to be an axon in these analyses. Each value represents the mean ± s.e.m. of at least 50–75 cells for each experimental condition. Asterisk represents value significantly different from that of the GFP-transfected group ( $P < 0.01$ ). ND, not detected.

reaching stage 3 (Figure 6B). As compared with EGFP alone or un-transfected cells, a significantly smaller fraction of βARKct-transfected cells reached stage 2 (17%) or stage 3 (4%) (Table I). Neurons transfected 12 h after plating seemed to be arrested in stage 2 (Figure 6B). This result is very similar to what was seen with loss of Tctex-1 function wherein most Tctex-1-suppressed neurons had segmented lamellipodia but neither typical neurites nor growth cones (Chuang *et al*, 2005).

We then performed gain-of-function studies to examine the phenotype of neurons overexpressing Gβ1. Primary hippocampal neurons were transfected 2 h after plating with

FLAG-Gβ1 and EGFP expression vectors. In contrast to cells expressing EGFP alone, a significantly greater number of FLAG-Gβ1-transfected neurons developed multiple long neurites (Figure 6A and Table I). Similar to the case of Gβ1 overexpression and as demonstrated previously (Chuang *et al*, 2005), Tctex-1 overexpression also elicited the same phenotype of multiple long neurites (Figure 6A and Table I), demonstrating that ectopic overexpression of either Gβ1 or Tctex-1 promotes neurite outgrowth. Coexpression of Tctex-1 along with the Gβγ-sequestering reagent βARKct seems to partially revert the phenotype induced by βARKct by 24 h after transfection (Figure 6A, Table I and Supplementary Figure 1).

**Gβγ overlaps with the 'dynein-free' pool of Tctex-1 and regulates assembly of Tctex-1 into the dynein motor complex**

Previous studies demonstrated that Tctex-1-mediated neurite outgrowth proceeds via a dynein-independent mechanism (Chuang *et al*, 2005). However, how dynein-bound and dynein-free pools of Tctex-1 are regulated in neurons remains unclear. We are interested in testing whether the Gβ-Tctex-1 complex may modulate the partition of Tctex-1 into dynein-associated and dynein-free pools. Toward this end, we first examined whether Gβγ overlaps with the dynein-associated or dynein-independent pool of Tctex-1. Using velocity density gradient sedimentation of lysates generated from embryonic E15 mouse brains, we demonstrated that, as shown previously, in addition to co-sedimenting with the DIC-containing, 19–20S fractions, Tctex-1 can also be found in the dynein-free, lighter-density fractions (Figure 7A). Interestingly, we show that the majority of Gβ-containing fractions overlap with the lighter, non-DIC containing fraction of Tctex-1. Very little, if any, Gβ can be found in the DIC-containing, higher-density fractions (Figure 7A).

Tctex-1 binding to DIC is required for its incorporation into the dynein motor complex. We observed that all known Gβ isoforms contain a DIC-like, consensus basic Tctex-1-binding motif (R/K-R/K-X-R/K) (Figure 3B) and (Mok *et al*, 2001). Since Gβ contains the same Tctex-1-binding motif as DIC, we investigated whether Tctex-1 can simultaneously bind to Gβ and DIC. We investigated the effect of overexpression of full-length FLAG-tagged Gβ1 on the ability of Tctex-1 to interact with DIC. Figure 7B shows that Gβ1 overexpression results in dramatically reduced Tctex-1 binding to endogenous DIC in HEK 293 cells. We further assessed the DIC-Tctex-1 interaction in the presence of a Gβ-peptide corresponding to amino acids 40–57 of Gβ1, which includes the basic Tctex-1-binding motif and surrounding residues. As shown in Figure 7C, the presence of increasing concentration of the Gβ-peptide leads to decreased amounts of Tctex-1 that can be co-immunoprecipitated with DIC in an anti-DIC pull down.

**Discussion**

The recent discoveries of novel and non-canonical modes of G protein signaling and regulation have expanded the

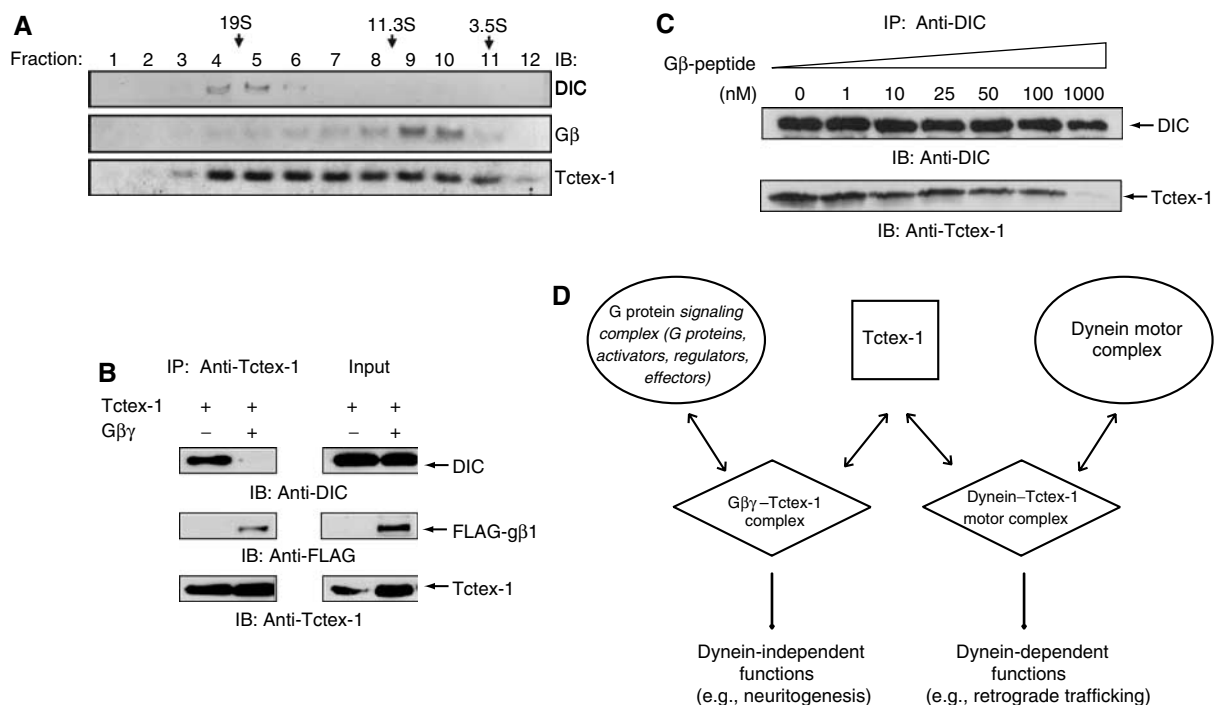


**Figure 7** Gβ overlaps with dynein-free pool of Tctex-1 and competes with DIC for Tctex-1 binding. (A) Gβ co-sediments with the dynein-free lighter fractions of Tctex-1. Homogenates from E15 mouse brain were sedimented in a 5–20% linear sucrose gradient. Each fraction was analyzed by SDS-PAGE and immunoblotted with the indicated antibodies. (B) Coexpression of Gβγ along with Tctex-1 resulted in decreased amounts of DIC associated with Tctex-1. HEK cells were transfected with either Tctex-1 alone (lane 1) or cotransfected with Tctex-1 along with FLAG-Gβ1 (lane 2). Tctex-1 was immunoprecipitated with anti-Tctex-1 antibody and the immunocomplexes were analyzed with anti-DIC antibody (top), anti-FLAG antibody (middle) and anti-Tctex-1 antibodies (bottom). Total cell lysate (TCL) was subjected to direct Western analysis to show expression levels of DIC, FL-Gβ1 and Tctex-1 (right panel). (C) Competition of dynein-Tctex-1 interaction by Gβ-peptide. DIC was immunoprecipitated (IP) from lysates generated from HEK cells transfected with Tctex-1 cDNA. The DIC IP was titrated with increasing concentration of unlabeled Gβ-peptide (0–1000 nM) as indicated. The amino-acid sequence of the Gβ-peptide is provided in Materials and methods. As the concentration of the peptide increased, a decreasing amount of Tctex-1 was detected in the immune complex, as measured using an anti-Tctex-1 antibody. The filter was probed with anti-DIC antibody to demonstrate that equivalent amounts of DIC were immunoprecipitated. (D) Model of Gβγ-dependent regulation of dynein-free function of Tctex-1 in inducing neurite outgrowth. Tctex-1 binding to DIC is required for incorporation of Tctex-1 in the dynein motor complex. Tctex-1 has been shown to exist free of dynein in cells. The dynein motor function is dispensable for the ability of Tctex-1 to induce neuritogenesis in primary hippocampal neurons. In embryonic mouse brain lysates, Gβγ overlaps with the dynein-free fractions of Tctex-1. We propose that G protein βγ subunit, which contains the DIC-like Tctex-1-binding motif and competes with DIC for Tctex-1 binding, serves to regulate the dynein-free pool of Tctex-1. The Gβγ-Tctex-1 complex exists free of the dynein-Tctex-1 complex and regulates the dynein-independent function of Tctex-1.



classical repertoire of receptor-dependent G protein activation (Cismowski and Lanier, 2005; McCudden *et al*, 2005). AGS proteins are a functionally defined group of proteins that activate G protein signaling in the absence of a classical G protein-coupled receptor (GPCR). It has been proposed that AGS proteins play important roles in the generation or positioning of signaling complexes and may serve as alternative binding partners for G protein subunits. Notably, receptor-independent activation of G proteins has been implicated in proper positioning of the mitotic spindle and asymmetric cell division (Willard *et al*, 2004). Silencing of AGS3, a receptor-independent activator of G $\beta$  $\gamma$  signaling, resulted in defects in mitotic spindle orientation and cleavage plane determination of neural progenitors in the developing neocortex affecting neuronal cell fate (Sanada and Tsai, 2005). AGS2 was identified as a G $\beta$  $\gamma$ -binding protein and was shown to be identical to cytoplasmic dynein light-chain Tctex-1 (Takesono *et al*, 1999). Interestingly, Tctex-1 has been shown to have both dynein-dependent and dynein-independent functions, and there is biochemical evidence for a dynein-free pool of Tctex-1 (Tai *et al*, 1998; Chuang *et al*, 2005). It is completely unclear how the dynein-associated and dynein-free pools of Tctex-1 are maintained in the cell.

In this study, we have investigated the functional role of the AGS2/Tctex-1-G $\beta$  $\gamma$  complex. We demonstrate that both G $\beta$  $\gamma$  and Tctex-1 distribute in primary hippocampal neurons similarly within the cell body and in the growth cone of the future axon of differentiated neurons. As with Tctex-1, ectopic expression of G $\beta$  $\gamma$  induces multiple neurites, whereas interfering with G $\beta$  $\gamma$  signaling, using a G $\beta$ -sequestering reagent  $\beta$ ARKct, inhibits neurite outgrowth. We demonstrate that all known isoforms of G $\beta$  contain a DIC-like Tctex-1-binding motif and ectopic expression of G $\beta$ 1 interferes with the Tctex-1-DIC interaction. Moreover a G $\beta$ -peptide, spanning the Tctex-1-binding motif, competes with DIC for Tctex-1 binding, suggesting that G $\beta$  $\gamma$ -Tctex-1 interaction may modulate the dynein-Tctex-1 motor complex formation. Since the neurogenic effects of Tctex-1 are dynein motor activity independent, G $\beta$  $\gamma$  binding to Tctex-1 provides a mechanistic model for recruiting and maintaining a dynein-free pool of Tctex-1 and the role of this complex in Tctex-1-mediated neurite outgrowth.

#### Dual role of Tctex-1

Tctex-1 has been identified as a light-chain subunit of the cytoplasmic dynein motor complex (Vallee *et al*, 2004), where it acts as a cargo adaptor for the dynein motor (Tai *et al*, 1999). However, Tctex-1 seems to have two functional roles—one as a dynein motor component and the second as a dynein-independent regulator of cell fate. A dynein-free pool of Tctex-1 has been confirmed biochemically (Tai *et al*, 1998; Li *et al*, 2004). Dynein motor activity is dispensable for Tctex-1-mediated modulation of cortical microfilament dynamics and Rac1 activity in embryonic hippocampal neurons (Chuang *et al*, 2005). G $\beta$  $\gamma$  overlaps with dynein-free, less-dense fractions of Tctex-1 in embryonic brain lysates, suggestive of a dynein-independent role for the G $\beta$  $\gamma$ -Tctex-1 complex.

We have identified a common Tctex-1-binding motif, which was initially defined by comparing the minimum Tctex-1-interacting sequence of DIC with other known Tctex-1-interacting proteins (Mok *et al*, 2001), in all known

isoforms of G $\beta$ . The sequence alignment demonstrates that all known G $\beta$  subunits contain a DIC-like Tctex-1-binding motif. This region of G $\beta$  maps to the outermost  $\beta$ -strand of the seventh blade of the G $\beta$  propeller and has been previously shown to contain residues important for interaction with other known G $\beta$  $\gamma$  effectors, including PLC $\beta$ 2 and RACK1 (Panchenko *et al*, 1998; Buck and Iyengar, 2001; Chen *et al*, 2005). A second Tctex-1-binding motif has also been identified, although it was often found that gaps of varying lengths had to be inserted and parts of the sequence were missing (Sugai *et al*, 2003). Overall, Tctex-1-interacting proteins fall into following three broad subsets: proteins that contain only the core basic R/K-R/K-X-X-R/K consensus motif; proteins that contain only the second Tctex-1-binding motif and proteins that contain both binding motifs. G $\beta$  belongs to the first subset. We show both full-length G $\beta$  and a G $\beta$ -peptide, corresponding to amino acids derived from G $\beta$ 1 spanning the putative Tctex-1-binding motif, compete with DIC for Tctex-1 binding.

According to a model proposed by Wu *et al* (2005), DIC and cargo proteins would bind to opposite ends of the Tctex-1 dimer. However, Tctex-1-interacting proteins that contain only the core, DIC-like Tctex-1-binding motif, present a paradox, since these proteins must interact with Tctex-1 in the same region as DIC (Wu *et al*, 2005). It is therefore unclear whether proteins containing only the same core binding motif can be bound to the dynein-Tctex-1 complex and serve as cargo for transport by the dynein motor complex. Our data demonstrate that G $\beta$  $\gamma$  competes with DIC for Tctex-1 binding. We propose that the G $\beta$  $\gamma$ -Tctex-1 complex cannot itself be incorporated in the dynein motor complex. However, G $\beta$  $\gamma$  regulates incorporation of Tctex-1 into the dynein motor complex and thereby regulates dynamics of the dynein-free pool of Tctex-1. Structural studies of the Tctex-1-G $\beta$  $\gamma$  co-complex are underway to help clarify whether G $\beta$  and DIC can simultaneously bind Tctex-1.

#### Role of G $\beta$ $\gamma$ and Tctex-1 in regulating neuronal differentiation

Several lines of evidence suggest a role for the G $\beta$  $\gamma$ -Tctex-1 interaction in neuronal differentiation. Tctex-1 was recently shown to play an important role in multiple steps of neuronal development, including neurite sprouting and extension, axonal polarity and dendritic arbor elaboration (Chuang *et al*, 2005). Moreover, Tctex-1 is highly abundant in fetal brains and in postmitotic young neurons in adult brain (Chuang *et al*, 2001). We report that G $\beta$  $\gamma$  and Tctex-1 share overlapping expression patterns in primary hippocampal neurons. Both Tctex-1 and G $\beta$  $\gamma$  localize in the growth cone of the axons in stage 3 neurons. Disruption of Tctex-1 expression and interfering with G $\beta$  $\gamma$  function results in inhibition of neurite outgrowth, whereas ectopic expression of G $\beta$  $\gamma$  and Tctex-1 results in multiple axon-like long neurites. Moreover, interfering with G $\beta$  $\gamma$  function partially reduced the ability of Tctex-1 to induce its neurogenic effects, suggesting that the G $\beta$  $\gamma$ -Tctex-1 complex is required for full activity of Tctex-1. But how does G $\beta$  $\gamma$  regulate Tctex-1-induced neuronal effects? We show that G $\beta$  $\gamma$  competes with DIC for Tctex-1 binding and thus regulates the incorporation of Tctex-1 into the dynein motor complex. Since motor activity is dispensable for Tctex-1-mediated neurite outgrowth and it is the dynein-free pool of Tctex-1 that promotes its neurogenic

effects, according to our model (see Figure 7D), G $\beta\gamma$  binding to Tctex-1 prevents its incorporation into the dynein complex and thereby promotes its dynein-independent activity.

Ectopic expression of Tctex-1 mostly reverts the dramatic inhibition of neurite outgrowth observed in the presence of the G $\beta\gamma$ -sequestering reagent,  $\beta$ ARKct. Since both G $\beta\gamma$  and Tctex-1 interact with several proteins and regulate various signaling pathways, it is probable that the G $\beta\gamma$ -Tctex-1 complex could be one of several signaling complexes leading to regulation of neurite induction and neuronal differentiation. For example, Tctex-1 stimulation of actin dynamics in neurons seems to be Rac dependent (Chuang *et al*, 2005). Tctex-1 may directly interact with a Rac-GEF to modulate Rac activity. Rho family GTPases are key regulators of actin dynamics that lead to actin-based assemblies associated with the structure and motility of cells. Rho GTPases have emerged as common regulators of actin dynamics that drive growth cone motility. The activity of Rho GTPases is regulated by a variety of proteins that either promote GTP uptake (GEFs) or stimulate hydrolysis (GAPs). Sequential activation of Rap1B and Cdc42 was shown to be essential for axonal specification and the establishment of neuronal polarity in hippocampal neurons (Schwamborn *et al*, 2004, 2006). G $\beta\gamma$  drives the membrane recruitment and activation of PAK-associated PIX $\alpha$ , an exchange factor for Cdc42 (Li *et al*, 2003). This G $\beta\gamma$ -PAK1/PIX $\alpha$ /Cdc42 complex and phosphatidylinositol 3-kinase (PI3K) product PI(3,4,5)P<sub>3</sub> (PIP<sub>3</sub>) were demonstrated to be essential for actin polymerization at the leading edge and persistent directional migration of myeloid cells (Li *et al*, 2003). G $\beta\gamma$  subunit might serve to link extracellular cues to localized regulation of actin and microtubule dynamics. Rho GTPases and their modulators provide a direct link between cell surface receptors, including growth factor receptors and GPCRs, and cytoskeletal rearrangements, leading to cell motility and cell polarity.

Tctex-1, but not the other dynein subunits, is highly abundant in the two germinal zones of adult brain, namely dentate gyrus and subventricular zone (SVZ) (Dedesma *et al*, 2006). In the developing neocortex, neural stem cells at the ventricular zone (VZ) either symmetrically divide into two identical daughter cells (e.g., progenitors or postmitotic neurons), or asymmetrically divide into one progenitor and one postmitotic neuron. Sanada and Tsai (2005) showed that perturbation of G $\beta\gamma$  signaling resulted in significantly decreased frequency of asymmetric cell division causing an overproduction of postmitotic neurons at the expense of mitogenic neural stem cells (Sanada and Tsai, 2005). Disruption of AGS3, which binds to G $\alpha$ i-GDP, preventing the reassociation of G $\beta\gamma$  with G $\alpha$  to reform the heterotrimer, leads to a phenotype resembling perturbation of G $\beta\gamma$  signaling (Sanada and Tsai, 2005). In the cortical neural progenitor cells, interfering with G $\beta\gamma$  function resulted in defects associated with mitotic spindle orientation and cleavage plane determination. But exactly how G $\beta\gamma$  regulates mitotic spindle alignment and cleavage orientation and thereby asymmetric cell division of neural stem cells is still unclear. Taken together, it can be concluded that G proteins and molecules that regulate G protein signaling are important players in neuronal development. We show specifically that G $\beta\gamma$  and Tctex-1, which individually are important in various pathways involving neuronal development, act in concert to regulate neuritogenesis.

## Materials and methods

### Antibodies, chemical reagents and plasmid constructs

DIC mAb (clone 74.1) was obtained from Chemicon (Temecula, CA), anti-FLAG pAb and tyrosinated-tubulin (Tyr-Tubulin) (clone TUB1A2) mAb from Sigma-Aldrich (St Louis, MO), anti-pan G $\beta$  antibody, (cat. no. sc-378), which recognizes all G $\beta$  isoforms and anti-G $\gamma$ 1 and anti-G $\gamma$ 2, from Santa Cruz Biotechnology (Santa Cruz, CA), horseradish peroxidase (HRP)-conjugated anti-mouse and anti-rabbit IgG from Jackson ImmunoResearch Laboratories (Bar Harbor, ME) and Alexa 488-conjugated goat anti-rabbit and Alexa 594-conjugated goat anti-mouse secondary antibodies from Invitrogen (Carlsbad, CA). Isopropyl-1-thio- $\beta$ -D-galactopyranoside (IPTG) was obtained from US Biological (Swampscott, MA). Affinity-purified anti-Tctex-1 pAb was described in Tai *et al* (1998), and additionally, an anti-Tctex-1 mAb antibody was also generated (see Supplementary Figure 2, and J-Z Chuang and C-H Sung, unpublished data). Untagged Tctex-1 cloned into pET-3a was a gift from Dr Zhang (Mok *et al*, 2001). Expression vectors encoding EGFP, pEGFP-C1 (Clontech Laboratories Inc., Mountain View, CA), untagged and FLAG-tagged Tctex-1 (Chuang *et al*, 2001), untagged and FLAG-tagged G $\beta$ 1 and FLAG-tagged G $\beta$ 2, G $\beta$ 3, G $\beta$ 5 and G $\beta$ 5L (UMR cDNA Resource Center, www.cdna.org), and control vector pcDNA3.1 (+) (Invitrogen, Carlsbad, CA) were used.

### Peptide synthesis and purification

Unlabeled G $\beta$ -peptide, <sup>40</sup>VGRIQMTRRTRLRGLAK-<sup>57</sup> and labeled G $\beta$ -peptide, C(MIANS)-<sup>40</sup>VGRIQMTRRTRLRGLAK-<sup>57</sup> [MIANS = 2-(4'-maleimidylanilino)naphthalene-6-sulfonic acid] (corresponding to the amino-acid sequence of G $\beta$ 1) were obtained from the Proteomics Resource Center of Rockefeller University. Peptides were synthesized using F-moc amino acids and had amidated C-terminus. Molecular mass was confirmed by MALDI mass spectrometry, purified to greater than 95% purity by reverse-phase high-performance liquid chromatography (RP-HPLC) and was highly soluble in water.

### Protein expression and purification

Tctex-1 was expressed and purified both as a GST-tagged protein as well as an untagged protein as described in Mok *et al* (2001). Briefly, a three-step FPLC-based column chromatography procedure was used. pET-3a vector encoding mouse Tctex-1 cDNA transformed into *Escherichia coli* BL21(DE3) host cells and Tctex-1 expression was induced by the addition of 400  $\mu$ M IPTG. The cells were harvested and lysed 3 h after induction and the cleared lysate was loaded onto a HiPrep 16/10 DEAE Sepharose (GE Healthcare) column and the protein was eluted with a linear NaCl gradient of 0–0.3 M. Fractions containing Tctex-1 were pooled, concentrated and loaded onto a sizing column (HiLoad 16/60 Superdex 75 gel filtration column) and excess salt was removed by desalting chromatography (Hi Prep 26/10 desalting column). Fractions from the desalting column were loaded on to a MonoQ HR 5/5 and eluted with a gradient of 0–0.35 M NaCl. The purified Tctex-1 was dialyzed and snap frozen in working aliquots and stored at  $-80^{\circ}\text{C}$ . Transducin (G $\alpha\beta\gamma$ ) was purified from frozen bovine retinas (Min *et al*, 1993; Marin *et al*, 2000). The purified proteins were snap frozen in working aliquots and stored at  $-80^{\circ}\text{C}$ .

### Fluorescence anisotropy

Interaction between MIANS-labeled G $\beta$ -peptide and Tctex-1 was monitored by fluorescence anisotropy. Anisotropy values were measured as described previously (Krishna *et al*, 2002). Briefly, the peptide was excited at 325 nm and the fluorescence anisotropy was measured in the absence or presence of Tctex-1 at 440 nm. Ludox was used as a standard in the anisotropy experiments (with an anisotropy value of  $\sim 0.97$ ).

### Cell culture and transfection

HEK 293 cells were grown in Dulbecco's modified Eagle's medium (DMEM; Invitrogen) supplemented with 10% (v/v) fetal calf serum. All cell cultures were maintained in 5% CO<sub>2</sub> at 37 $^{\circ}\text{C}$ . For immunoprecipitation assays, HEK293 cells were plated in 10-cm plates and transfected with 3.5  $\mu$ g DNA/plate using Lipofectamine Plus (Invitrogen). Cell extracts were generated 48 h after transfection.

**Immunoprecipitation and peptide competition assay**

Cells were lysed in lysis buffer (50 mM Tris-HCl, pH 7.5, 150 mM NaCl, EDTA, 2 mM EDTA, 1.0% (v/v) Triton X-100) plus protease inhibitor mixture (1 mM phenylmethylsulfonyl fluoride, 2  $\mu$ g/ml aprotinin, 2  $\mu$ g/ml leupeptin and 0.7  $\mu$ g/ml pepstatin). Cell lysates were cleared by centrifugation and the supernatant fractions were then incubated with antibody and Protein A-agarose beads (Repligen, Cambridge, MA) for 2 h at 4°C. For G $\beta$ -peptide competition assay, cell lysates were incubated with either anti-DIC antibody alone or in the presence of increasing concentration of unlabeled G $\beta$ -peptide (1, 10, 25, 50, 100 or 1000 nM). The immunoprecipitates were washed three times with cold lysis buffer. The proteins were released from beads by boiling in SDS sample buffer and separated by SDS-PAGE. Proteins were transferred to nitrocellulose and detected using anti-G $\beta$  (1:1000), anti-Tctex-1 (1:2000), anti-FLAG (1:5000) or anti-DIC (1:1000) antibodies.

**Culture and immunofluorescence analyses of hippocampal neurons**

Cultures of dissociated embryonic hippocampal neurons were prepared as described previously (Goslin and Banker, 1991; Chuang *et al*, 2005). Briefly, embryonic E18 rat brains were dissected, the isolated hippocampi were incubated in 1  $\times$  HBSS (Invitrogen) containing 0.25% trypsin for 15 min at 37°C and dissociated by pipetting in plating medium (minimum essential medium (MEM) supplemented with 10% horse serum, glucose and 100 U/ml penicillin/streptomycin; Invitrogen). Freshly trypsin-dissociated neurons were plated onto glass coverslips coated with poly-L-lysine (Sigma P2636) and cultured at 37°C and 5% CO<sub>2</sub>. For endogenous expression analysis, neurons were allowed to attach to the substrate followed by incubation in maintenance medium (MEM supplemented with ovalbumin, B27 and N2.1 supplement, pyruvate, and 100 U/ml penicillin/streptomycin; Invitrogen). Neurons were fixed at 1–3 days *in vitro* (d.i.v.) with 4% paraformaldehyde/sucrose solution in phosphate-buffered saline (PBS) for 15 min at room temperature (RT) and processed for immunohistochemistry. For transfection studies, neurons were transfected either at 2 h after plating or 12 h after plating using Lipofectamine 2000 (Invitrogen) following the manufacturer's protocol, with minor adjustments. Total DNA amount for each transfection was kept constant using the empty backbone control vector, pcDNA3.1(+). Neurons were incubated with the DNA:lipid mixture for 2 h at 37°C and the medium was then removed and replaced with maintenance medium. Neurons were fixed at the indicated times and processed

for immunohistochemistry following published protocols (Chuang *et al*, 2005). Primary antibody was followed by goat anti-rabbit or anti-mouse secondary antibodies coupled to Alexa 488 or Alexa 594 (Invitrogen). The coverslips were mounted in Vectashield mounting medium (Vector Labs Inc., Burlingame, CA) with DAPI. All immunostained cells were analyzed either using a Zeiss confocal microscope or a Zeiss Axiovert 200 M equipped with an AxioCam HR camera. At least three independent experiments were conducted for each manipulation and 50–100 cells on 15–40 coverslips were examined in each experiment. Different stages of neuritic development were classified based on established guidelines (Dotti *et al*, 1988; Chuang *et al*, 2005). Quantification of labeling intensities and morphometric analyses were carried out using Metamorph software (Universal Imaging Co., Downingtown, PA) as described (Chuang *et al*, 2005) and the images were processed using Adobe Photoshop.

**Velocity density gradient sedimentation**

Embryonic E15 mouse brains were harvested and rinsed with ice-cold PBS twice. Cells were broken using the Dounce homogenizer (Kimble Kontes, Vineland, NJ) with pestle A (10 times) followed by pestle B (20 times) in 1 ml PEM buffer (80 mM PIPES, pH 6.8, 1 mM EGTA, 1 mM MgSO<sub>4</sub>, 0.5 mM DTT and protease inhibitors) on ice. Homogenates were cleared by centrifugation at 2000 r.p.m. for 5 min to remove nuclei followed by centrifugation at 100 000 g at 4°C for 1 h. The high-speed supernatant fraction was fractionated in a 5–20% linear sucrose gradient in 11 ml of Tris-KCl buffer (20 mM Tris, pH 7.5, 50 mM KCl, 5 mM MgCl<sub>2</sub>, 0.5 mM EGTA, 0.5 mM DTT and protease inhibitors) using a SW41 Ti rotor (Beckman) at 32 000 r.p.m. in 4°C for 16 h. The S-values were determined by measuring the reflective index of each fraction.

**Supplementary data**

Supplementary data are available at *The EMBO Journal* Online (<http://www.embojournal.org>).

**Acknowledgements**

PS was supported earlier by the NIH Training Grant EY07138 and is currently a fellow of the Murray Foundation. TPS was formerly an Ellison Medical Foundation senior scholar. This work was supported in part by NIH EY11307 to C-HS and the Alene Reuss Memorial Trust and the Howard Hughes Medical Institute.

**References**

- Baas PW, Bister DW (2004) Slow axonal transport and the genesis of neuronal morphology. *J Neurobiol* **58**: 3–17
- Banker G (2003) Pars, PI 3-kinase, and the establishment of neuronal polarity. *Cell* **112**: 4–5
- Bradke F, Dotti CG (2000) Establishment of neuronal polarity: lessons from cultured hippocampal neurons. *Curr Opin Neurobiol* **10**: 574–581
- Buck E, Iyengar R (2001) Modular design of G $\beta$  as the basis for reversible specificity in effector stimulation. *J Biol Chem* **276**: 36014–36019
- Chen S, Lin F, Hamm HE (2005) RACK1 binds to a signal transfer region of G $\beta$  and inhibits PCLbeta 2 activation. *J Biol Chem* **280**: 33445–33452
- Chuang JZ, Milner TA, Sung CH (2001) Subunit heterogeneity of cytoplasmic dynein: differential expression of 14 kDa dynein light chains in rat hippocampus. *J Neurosci* **21**: 5501–5512
- Chuang JZ, Yeh TY, Bollati F, Conde C, Canavosio F, Caceres A, Sung CH (2005) The dynein light chain Tctex-1 has a dynein-independent role in actin remodeling during neurite outgrowth. *Dev Cell* **9**: 75–86
- Cismowski MJ, Lanier SM (2005) Activation of heterotrimeric G-proteins independent of a G-protein coupled receptor and the implications for signal processing. *Rev Physiol Biochem Pharmacol* **155**: 75–80
- Dedesma C, Chuang JZ, Alfinito PD, Sung CH (2006) Dynein light chain Tctex-1 identifies neural progenitors in adult brain. *J Comp Neurol* **496**: 773–786
- Dotti CG, Sullivan CA, Banker GA (1988) The establishment of polarity by hippocampal neurons in culture. *J Neurosci* **8**: 1454–1468
- Douglas MW, Diefenbach RJ, Homa FL, Miranda-Saksena M, Rixon FJ, Vittone V, Byth K, Cunningham AL (2004) Herpes simplex virus type 1 capsid protein VP26 interacts with dynein light chains RP3 and Tctex1 and plays a role in retrograde cellular transport. *J Biol Chem* **279**: 28522–28530
- Fukata Y, Kimura T, Kaibuchi K (2002) Axon specification in hippocampal neurons. *Neurosci Res* **43**: 305–315
- Goslin K, Banker G (1991) *Rat Hippocampal Neurons in Low-Density Culture*. The MIT Press: Cambridge, MA
- Hirokawa N (1998) Kinesin and dynein superfamily proteins and the mechanism of organelle transport. *Science* **279**: 519–526
- Humphrey W, Dalke A, Schulten K (1996) VMD: visual molecular dynamics. *J Mol Graph* **14**: 33–38, 27–38
- Kai N, Mishina M, Yagi T (1997) Molecular cloning of Fyn-associated molecules in the mouse central nervous system. *J Neurosci Res* **48**: 407–424
- King SM (2000) The dynein microtubule motor. *Biochim Biophys Acta* **1496**: 60–75
- Koch WJ, Hawes BE, Allen LF, Lefkowitz RJ (1994) Direct evidence that Gi-coupled receptor stimulation of mitogen-activated protein kinase is mediated by G $\beta$  activation of p21ras. *Proc Natl Acad Sci USA* **91**: 12706–12710
- Krishna AG, Menon ST, Terry TJ, Sakmar TP (2002) Evidence that helix 8 of rhodopsin acts as a membrane-dependent conformational switch. *Biochemistry* **41**: 8298–8309

- Lambright DG, Sondek J, Bohm A, Skiba NP, Hamm HE, Sigler PB (1996) The 2.0 Å crystal structure of a heterotrimeric G protein. *Nature* **379**: 311–319
- Lanier SM (2004) AGS proteins, GPR motifs and the signals processed by heterotrimeric G proteins. *Biol Cell* **96**: 369–372
- Li MG, Serr M, Newman EA, Hays TS (2004) The *Drosophila* tctex-1 light chain is dispensable for essential cytoplasmic dynein functions but is required during spermatid differentiation. *Mol Biol Cell* **15**: 3005–3014
- Li Z, Hannigan M, Mo Z, Liu B, Lu W, Wu Y, Smrcka AV, Wu G, Li L, Liu M, Huang CK, Wu D (2003) Directional sensing requires G beta gamma-mediated PAK1 and PIX alpha-dependent activation of Cdc42. *Cell* **114**: 215–227
- Machado RD, Rudarakanchana N, Atkinson C, Flanagan JA, Harrison R, Morrell NW, Trembath RC (2003) Functional interaction between BMPR-II and Tctex-1, a light chain of dynein, is isoform-specific and disrupted by mutations underlying primary pulmonary hypertension. *Hum Mol Genet* **12**: 3277–3286
- Marin EP, Krishna AG, Zvyaga TA, Isele J, Siebert F, Sakmar TP (2000) The amino terminus of the fourth cytoplasmic loop of rhodopsin modulates rhodopsin-transducin interaction. *J Biol Chem* **275**: 1930–1936
- McCudden CR, Hains MD, Kimple RJ, Siderovski DP, Willard FS (2005) G-protein signaling: back to the future. *Cell Mol Life Sci* **62**: 551–577
- Min KC, Zvyaga TA, Cypess AM, Sakmar TP (1993) Characterization of mutant rhodopsins responsible for autosomal dominant retinitis pigmentosa. Mutations on the cytoplasmic surface affect transducin activation. *J Biol Chem* **268**: 9400–9404
- Mok YK, Lo KW, Zhang M (2001) Structure of Tctex-1 and its interaction with cytoplasmic dynein intermediate chain. *J Biol Chem* **276**: 14067–14074
- Mou T, Kraas JR, Fung ET, Swope SL (1998) Identification of a dynein molecular motor component in Torpedo electroplax; binding and phosphorylation of Tctex-1 by Fyn. *FEBS Lett* **435**: 275–281
- Ohka S, Matsuda N, Tohyama K, Oda T, Morikawa M, Kuge S, Nomoto A (2004) Receptor (CD155)-dependent endocytosis of poliovirus and retrograde axonal transport of the endosome. *J Virol* **78**: 7186–7198
- Panchenko MP, Saxena K, Li Y, Charnecki S, Sternweis PM, Smith TF, Gilman AG, Kozasa T, Neer EJ (1998) Sites important for PLCbeta2 activation by the G protein betagamma subunit map to the sides of the beta propeller structure. *J Biol Chem* **273**: 28298–28304
- Pfister KK, Fisher EMC, Gibbons IR, Hays TS, Holzbaur ELF, McIntosh JR, Porter ME, Schroer TA, Vaughan KT, Witman GB, King SM, Vallee RB (2005) Cytoplasmic dynein nomenclature. *J Cell Biol* **171**: 411–413. 10.1083/jcb.200508078
- Sakato M, King SM (2004) Design and regulation of the AAA + microtubule motor dynein. *J Struct Biol* **146**: 58–71
- Sanada K, Tsai LH (2005) G protein betagamma subunits and AGS3 control spindle orientation and asymmetric cell fate of cerebral cortical progenitors. *Cell* **122**: 119–131
- Schwamborn JC, Fiore R, Bagnard D, Kappler J, Kaltschmidt C, Puschel AW (2004) Semaphorin 3A stimulates neurite extension and regulates gene expression in PC12 cells. *J Biol Chem* **279**: 30923–30926
- Schwamborn JC, Li Y, Puschel AW (2006) GTPases and the control of neuronal polarity. *Methods Enzymol* **406**: 715–727
- Schwamborn JC, Puschel AW (2004) The sequential activity of the GTPases Rap1B and Cdc42 determines neuronal polarity. *Nat Neurosci* **7**: 923–929
- Schwarzer C, Barnikol-Watanabe S, Thinnies FP, Hilschmann N (2002) Voltage-dependent anion-selective channel (VDAC) interacts with the dynein light chain Tctex1 and the heat-shock protein PBP74. *Int J Biochem Cell Biol* **34**: 1059–1070
- Sugai M, Saito M, Sukegawa I, Katsushima Y, Kinouchi Y, Nakahata N, Shimosegawa T, Yanagisawa T, Sukegawa J (2003) PTH/PTH-related protein receptor interacts directly with Tctex-1 through its COOH terminus. *Biochem Biophys Res Commun* **311**: 24–31
- Tai AW, Chuang JZ, Bode C, Wolfrum U, Sung CH (1999) Rhodopsin's carboxy-terminal cytoplasmic tail acts as a membrane receptor for cytoplasmic dynein by binding to the dynein light chain Tctex-1. *Cell* **97**: 877–887
- Tai AW, Chuang JZ, Sung CH (1998) Localization of Tctex-1, a cytoplasmic dynein light chain, to the Golgi apparatus and evidence for dynein complex heterogeneity. *J Biol Chem* **273**: 19639–19649
- Takesono A, Cismowski MJ, Ribas C, Bernard M, Chung P, Hazard III S, Duzic E, Lanier SM (1999) Receptor-independent activators of heterotrimeric G-protein signaling pathways. *J Biol Chem* **274**: 33202–33205
- Vallee RB, Williams JC, Varma D, Barnhart LE (2004) Dynein: an ancient motor protein involved in multiple modes of transport. *J Neurobiol* **58**: 189–200
- Waterman-Storer CM, Karki S, Holzbaur EL (1995) The p150Glued component of the dynactin complex binds to both microtubules and the actin-related protein cactin (Arp-1). *Proc Natl Acad Sci USA* **92**: 1634–1638
- Willard FS, Kimple RJ, Siderovski DP (2004) RETURN OF THE GDI: the GoLoco motif in cell division. *Annu Rev Biochem* **73**: 925–951
- Wu H, Maciejewski MW, Takebe S, King SM (2005) Solution structure of the tctex1 dimer reveals a mechanism for Dynein-cargo interactions. *Structure (Camb)* **13**: 213–223
- Yano H, Chao MV (2004) Mechanisms of neurotrophin receptor vesicular transport. *J Neurobiol* **58**: 244–257
- Yano H, Lee FS, Kong H, Chuang J, Arevalo J, Perez P, Sung C, Chao MV (2001) Association of Trk neurotrophin receptors with components of the cytoplasmic dynein motor. *J Neurosci* **21**: RC125